



Slope Angle as Indicator Parameter of Landslide Susceptibility in a Geologically Complex Area

Angelo Donnarumma, Paola Revellino, Gerardo Grelle, and
Francesco Maria Guadagno

Abstract

Slope angles are a key parameter in estimating susceptibility to developing earth flows. In this paper, slope angles are used to estimate potential unstable areas in a pilot sector of the Benevento province in (Southern Italy).

Since the study area is characterized by a complex lithological setting, landslide distribution was analyzed within four-groups of homogeneous litho-technical sequences. Slope angle frequency distributions were obtained from a landslide sample in accordance with the Weibull probability density distribution function. Their analysis shows that the largest occurrence of landslides fall within an interval of slope angles ranging from 9° to 14° . As field surveys confirm, the low frequency of instabilities on steeper slopes can be explained by a deficit of potentially involving materials, partially due to the presence of stony sequences. Consequently, the probability of failure was calculated only on slope angle ranges already affected by existing landslide phenomena.

Keywords

Earth flows • Weibull distribution • Southern Italy

Introduction

Assessment of the landslide susceptibility and identification of potentially landslide-prone areas have both experienced extensive advances in scientific literature. A variety of methods have been developed using deterministic and statistical approaches based on slope angle distribution. Statistical analysis is widely used mainly in large-scale previsions studies, as it allows for a better understanding of the relationship between landslide phenomena and predisposing factors. Furthermore it guarantees a lower degree of subjectivity in contrast to heuristic methods.

However, a key issue is represented by the definition of predictive models founded on statistical bases. The

assumptions on which these models are based, are only partially satisfied when the statistical analysis deals with discrete variables such as for example the slope angle. In this case, analyses carried out by Ohmori and Sugai (1995), Iwahashi et al. (2001, 2003), Korup (2005), Xiaoyi and Jianping (2006), Guzzetti et al. (2007) and Lee et al. (2008) were based on the assumption that landslide susceptibility does not monotonically increase with an increase in the slope angle.

Nevertheless, even though landslide evolution is largely connected to the steepness of the slope in geomorphologic environments dominated by slow movements (such as earth flows), it has to be taken into account that high slope angles do not always produce earth flows. High gradients can be often due to the presence of stony layers within sequences, which influence the behavior of the masses (Grelle et al. 2011b)

Based on the above considerations, this paper aims to analyze the influence of the slope angle in earth flow occurrences, which involve structurally and lithologically complex sequences. The study was applied to a pilot area of

A. Donnarumma (✉) • P. Revellino • G. Grelle • F.M. Guadagno
Department of Biological, Geological and Environmental Sciences,
University of Sannio, Via dei Mulini, 59/A, Benevento, Italy
e-mail: angelo.donnarumma@unisannio.it

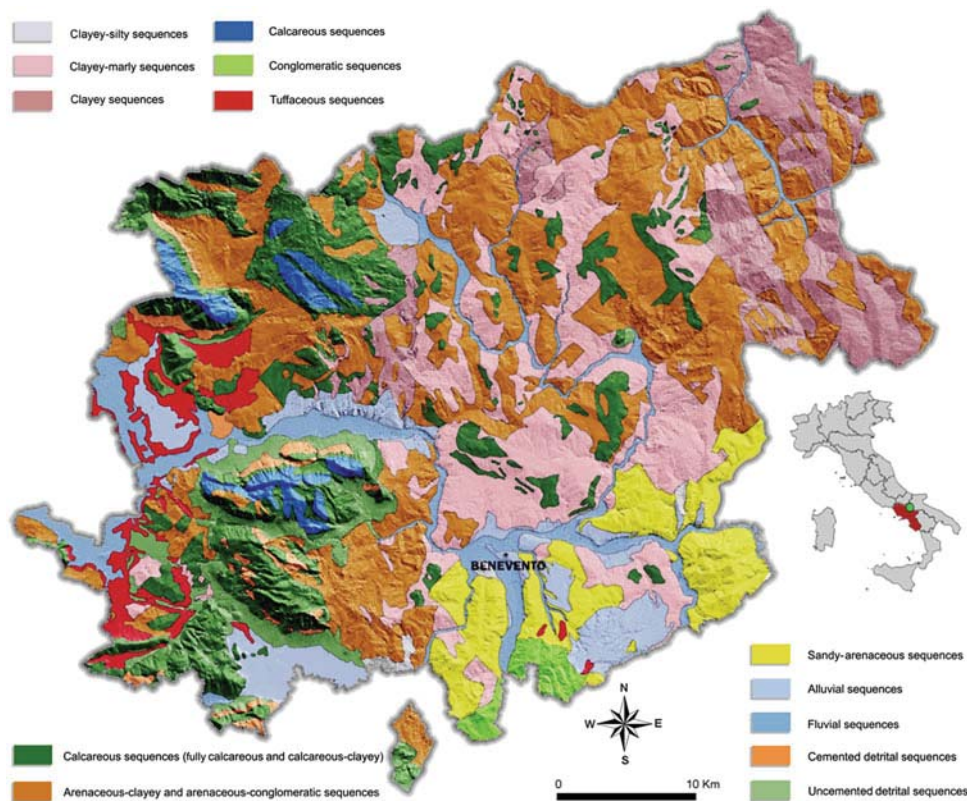


Fig. 1 DEM of the study area and litho-technical sequences outcropping

the Benevento province in Southern Italy, where considerable data relating to slope angles and lithological sequences was available (Guadagno et al. 2006).

Geological Features and Landslide Occurrence in the Study Area

The Province of Benevento (approximately 2,000 km²) has been historically affected by landslides prevalently of the earth flow type. Its morphological pattern is controlled by both the regional geo-structural setting, and the outcropping terrains which mainly consist of structurally complex formations (*sensu* Esu 1977).

Revellino et al. (2010) grouped these deposits into successions on the basis of their lithological and engineering-geological/geomechanical features (Fig. 1) in order to elucidate the relationship between landslides and the geological formations. Within these groups, the analysis was carried out only on the following sequences affected by earth flows: (1) Clayey sequences (CI); (2) Arenaceous-clayey-conglomeratic sequences (Ar-CI-Cg); (3) Clayey-silty sequences (CI-S) and Clayey-marly sequences (CI-M)

As regards landslides, recent studies carried out by Guadagno et al. (2006) and Revellino et al. (2010) led to an inventory of more than 3,100 earth flows, covering an

approximate area of 358 km², approximately 18 % of the entire surface area of the province (Fig. 2). By comparing Figs. 1, and 2, one can note that landslide phenomena are mainly connected to CI, Ar-CI-Cg, CI-S and CI-M litho-technical sequences.

Landslide distribution activity (*sensu* WP/WLI 1993) is generally advancing, except in the source area where it is retrogressive.

Moreover, large earth flows usually affect the full slope length, even though smaller and secondary phenomena, which have often different directions and velocities, as highlighted in the literature for similar instabilities (e.g. Corominas et al. 2005; Lollino et al. 2003), take place within the main landslide body. Usually, reactivations involve the full landslide bodies or limited sectors during long and intense storms.

Probability of Failure and Landslide Susceptibility

Scientific Background

Parametric statistical analysis is well suited to addressing landslide susceptibility assessments of geomorphologic environments dominated by recurrent slope instabilities. The experimental results obtained by PWRI (1976), Ohmori

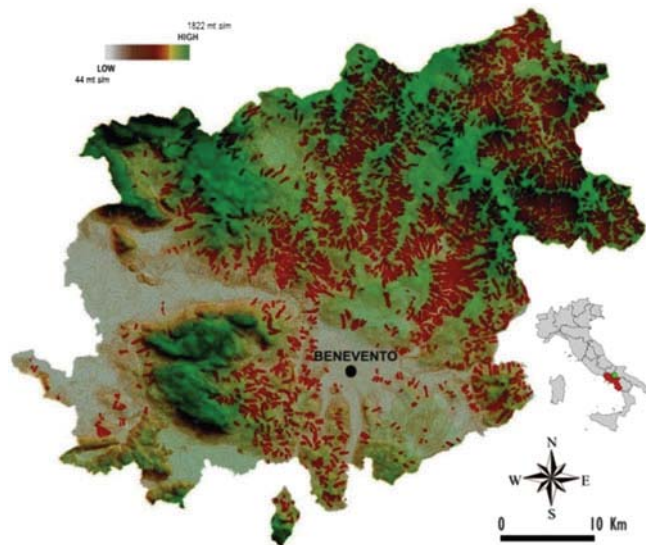


Fig. 2 Landslide distribution on DEM of the study area

and Sugai (1995) and Iwahashi et al. (2003) show that the distribution of the mean slope angle of a landslide population fits a sub-optimal Gaussian function. From a probabilistic point of view, the application of statistical-mathematical algorithms to slope angle data provides an estimate of slope failure proneness.

Since we deal with Gaussian distributions, the Probability Density Functions (PDFs) of Weibull (Weibull 1951) could be well applied, being that the mode angles for whole landslide masses varied in relation to the local geology (Iwahashi et al. 2001).

The mathematical structure of the 2- and 3-parameter Weibull PDFs, respectively, is defined by:

$$f(\alpha) = \left(\frac{\beta \alpha^{\beta-1}}{\eta^\beta} \right) \exp \left\{ - \left(\frac{\alpha}{\eta} \right)^\beta \right\}, \quad \alpha > 0 \quad (1)$$

$$f(\alpha) = \left(\frac{\beta}{\eta} \right) \left(\frac{\alpha - \gamma}{\eta} \right)^{\beta-1} \exp \left\{ - \left(\frac{\alpha - \gamma}{\eta} \right)^\beta \right\} \quad (2)$$

where α is the slope angle, β is the shape parameter, η is the scale parameter and γ is the location parameter. Each is a positive number.

As described by Iwahashi et al. (2003):

- β controls the shape of the function. If $\beta = 1$, the Weibull distribution coincides with exponential distribution. If $\beta > 1$, the Weibull distribution shows one peak on a probability density function graph. The situation, $\beta < 1$, indicates early failures; $\beta = 1$ indicates random failures. $\beta > 1$ implies wear-out failures.

- η controls the expansion and the reduction of the probability density function graphs, and moving the peak position, η indicates the theoretical mode of a failure. Iwahashi et al. (2003) clarified that the more fine-grained the geology, the smaller the value of η would thus result;
- γ controls the parallel movement of probability density function graphs.

The cumulative Weibull distribution function $F(A)$ (3) defines the probability of failure (Iwahashi et al. 2003). $F(A)$ is defined by the following equation:

$$F(A) = P(A < \alpha) = \sum_{\alpha_i < \alpha} P(A = \alpha_i) \quad (3)$$

Probability Density of the Slope Angle (α)

In order to investigate the evolutive character of the instabilities, a PDF of the slope angle (α) was computed in terms of landslides area. A 2-parameter Weibull model was thus applied allowing the PDF of α and the analysis of its spatial distribution to be determined.

Slope angle data was extracted from 1:5,000 scale maps by using an Arcview GIS Platform (ESRI 1999) implemented with Spatial Analyst and Analyst 3D modules. A count map of 10×10 m was used to sample the angle distribution.

The data binning was preliminarily made with 1-size, non zero intervals and was characterized by small dispersion. The PDF of α ($p(\alpha)$) was obtained by dividing the area of each interval by its own amplitude. More specifically, we fixed 0° as the starting point of the binning procedure and then we extracted the counts in each bin of a 1° amplitude:

$$p(\alpha) = \frac{1}{A_{LT}} \frac{\delta A_L}{\delta \alpha} \quad (4)$$

where δA_L is the landslide area between α and $\alpha + \delta \alpha$ and A_{LT} is the full landslide area. Equation (4) is normalized as follows:

$$\int_0^{\alpha/2} p(\alpha) d\alpha = 1 \quad (5)$$

The semi-logarithmic graphs (Fig. 3) show the α PDF of the landslides inventoried in the study area. By investigating the behavior of the PDFs, it was possible to note that the data set presents a double trend. The first, corresponding to the lower angles, has a positive correlation; the second, corresponding to the higher values, has a negative

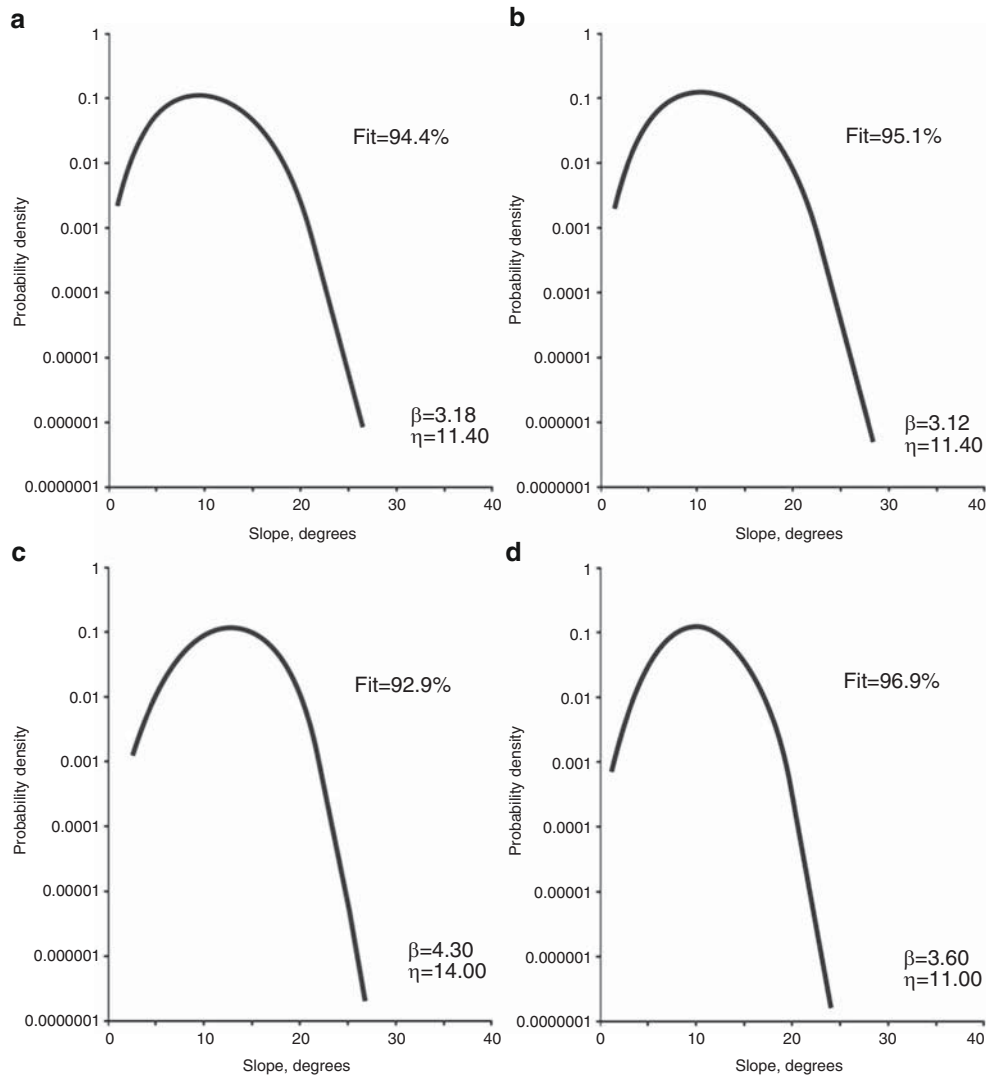


Fig. 3 Probability density function versus slope angle in the landslide area for each litho-technical sequence analyzed: (a) Clayey sequences, *CI*; (b) Arenaceous-clayey-conglomeratic sequences, *Ar-CI-Cg*; (c) Clayey-silty sequences, *CI-S*; (d) Clayey-marly sequences, *CI-M*

correlation. In particular, by approaching the peak, the values strongly decrease. In this way, it was possible to identify the slope sectors where landslides are spatially distributed.

Moreover, the PDFs obtained for each litho-technical sequence show peak values between 9–11°, 11–13° and 14–16° where landslides involved *CI* and *CI-M* (Fig. 3a, d), *Ar-CI-Cg* (Fig. 3b) and *CI-S* (Fig. 3c) respectively.

Probability Distribution of the Slope Angle (α)

In order to analyze the evolutive trend of slopes induced by instabilities, the spatial distributions of α were compared in both landslide and stable areas. Data was normalized in relation to the max of the two curves, allowing the range of the probability distribution variability to be restricted between 0 and 1.

As shown in Fig. 4a, b, which refer to sequences where the stony component is lacking or poorly present, data appears to be univocally distributed in terms of trend and peak values, being the curves fully overlapped (the average shift is: 5.97 % and 7.52 %, respectively). This result could highlight the fact that the slope steepness was reduced by extreme landslide processes. Indeed, in these areas, the Landslide Index, calculated as the percentage of the area affected by landslide events for a 1 km² grid for the whole province, is even more than 70 % (Revellino et al. 2010).

On the contrary, the data-set distributions of Fig 4c, d show a poor agreement of the peak values, which are significantly shifted, and a poor overlapping of the curves (the average shift is: 26.79 % and 13.78 %, respectively), above all in the case of *CI-S* sequences (Fig. 4c). Moreover, distribution tails also display a different behavior, which might be influenced by the poor number of events

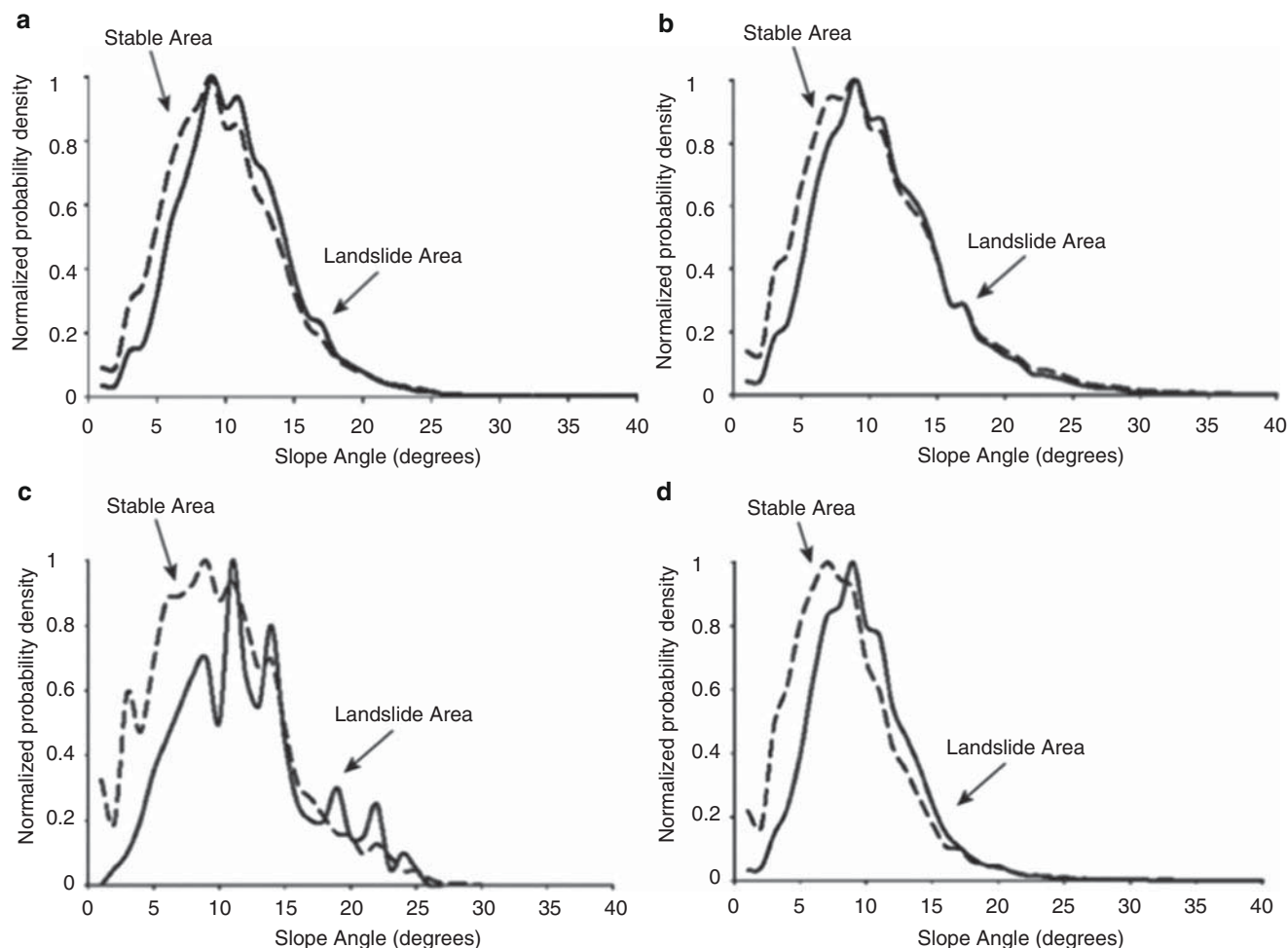


Fig. 4 Area probability density distribution, normalized in relation to the peak, vs slope angles of both landslides and stable area: (a) Clayey sequences, *Cl*; (b) Arenaceous-clayey-conglomeratic sequences, *Ar-Cl-Cg*; (c) Clayey-silty sequences, *Cl-S*; (d) Clayey-marly sequences, *Cl-M*

inventoried in this geological context too. As regards *Cl-S* and *Cl-M* sequences, landslide area distributions show prevailing slope angles around 10–12°. On the other hand, distributions of the stable areas are characterized by angles between 7° and 9°.

As confirmed by field surveys, it should be noted that landslide source areas are slowly evolving where the stony terrains are prevailing at the top of the sequence involved in landsliding. This field evidence is supported by the distributions of Fig. 5, where slope angles of the landslide source areas are compared with those of the respective channels.

Excluding the analysis on the *Cl-S* sequence, which could be influenced by the poor statistic representativeness of data due to the exiguous number of landslides recorded (# 14), the remaining sequences are characterized by distributions (Fig. 5) that are almost unchanged with respect to those in Fig. 4.

In the case of the *Cl-M* sequence, the α distribution of the source area is only slightly overlapped and shifted with

respect to the slope angle distribution of the entire landslide area. In addition, the peak values of the α probability density of the source areas are significantly higher (13–15°) with respect to those of the channel areas (8–9°). This could probably be related to the geo-mechanical resistance offered by the stony component that, in these sectors, constrains failure along the pre-existing weak surfaces such as fractures or bedding joints (Grelle et al. 2011b). The result is a slow and irregular retrogression, locally influenced by the fracture pattern of the stony terrain. The consequence is high evolutive control on the distribution of the activity as demonstrated by Revellino et al. (2010).

Probability of Failure

A statistical analysis of the frequency-mean slope angle relationship was carried out in order to define the probability of failure. The data fitting was performed by using the 3-parameter Weibull density function (Fig. 6). The result

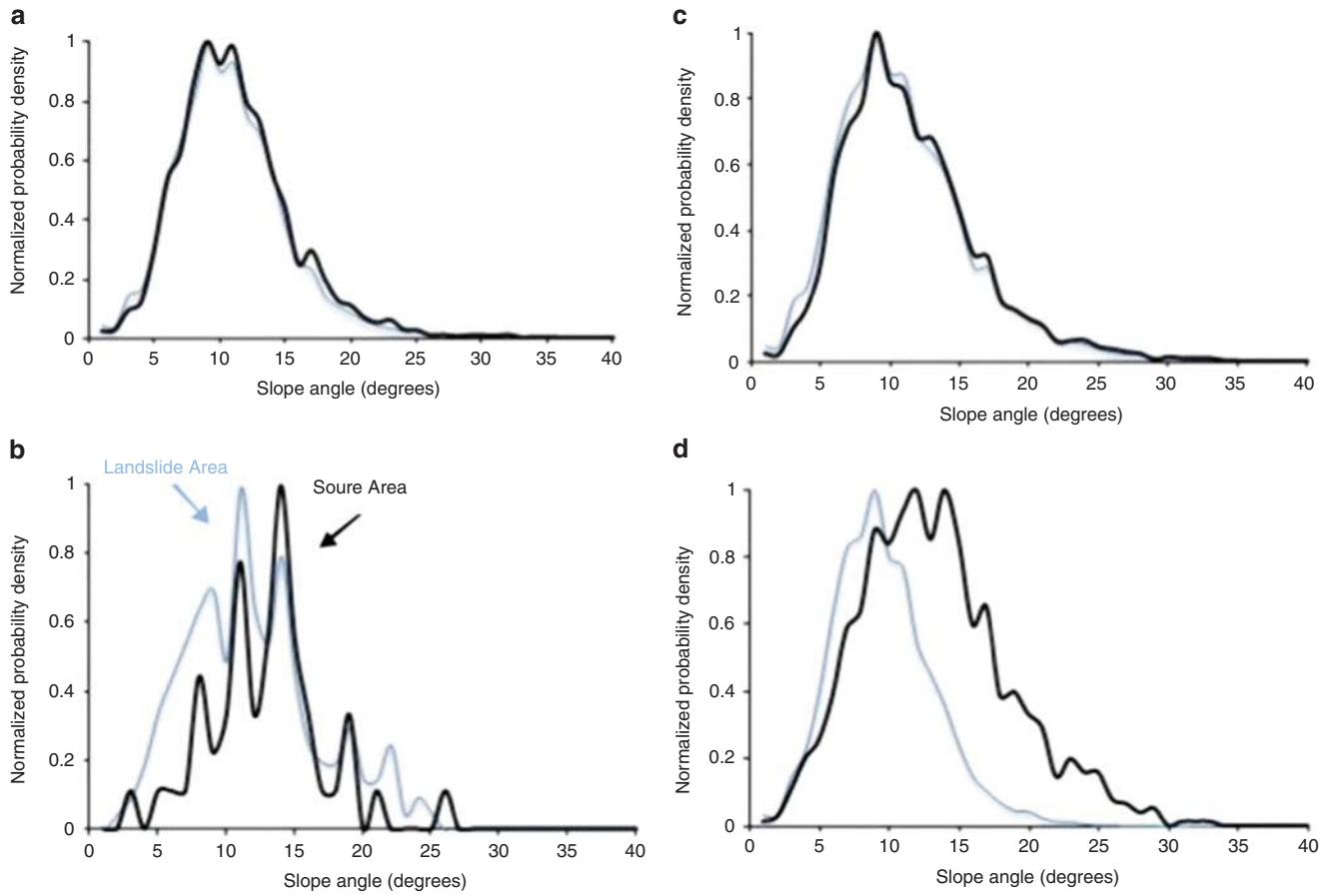


Fig. 5 Area probability density distribution, normalized in relation to the peak, vs slope angles of both landslides and source areas: (a) Clayey sequences, *Cl*; (b) Arenaceous-clayey-conglomeratic sequences, *Ar-Cl-Cg*; (c) Clayey-silty sequences, *Cl-S*; (d) Clayey-marly sequences, *Cl-M*

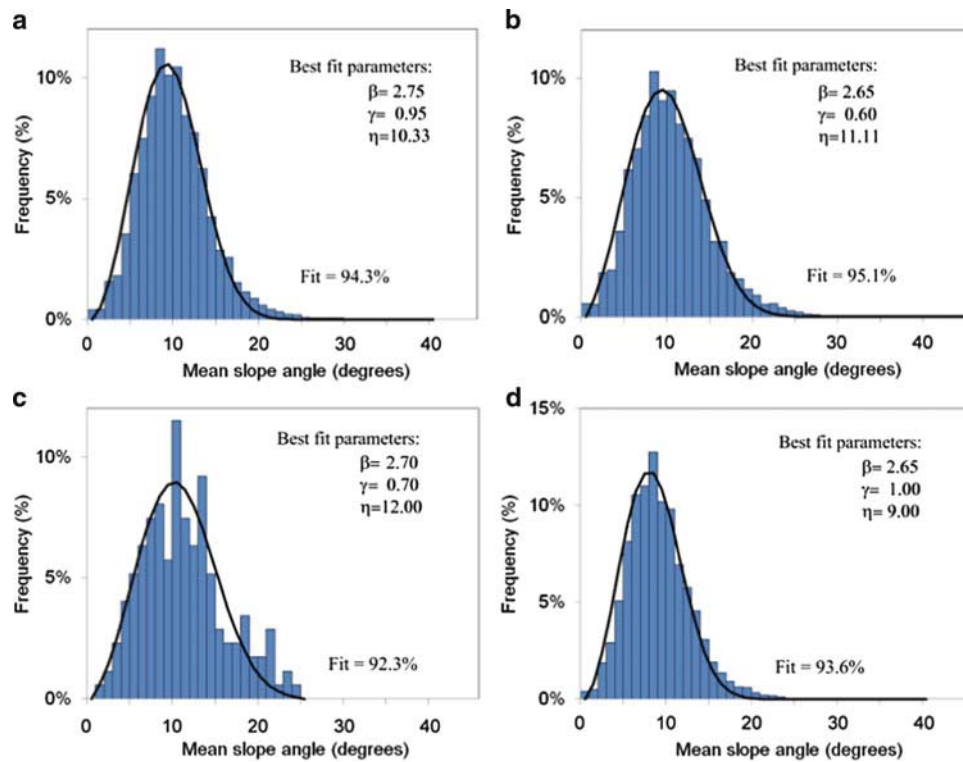


Fig. 6 Mean slope-angle frequency distributions of landslides for each geological sequence: (a) Clayey sequences, *Cl*; (b) Arenaceous-clayey-conglomeratic sequences, *Ar-Cl-Cg*; (c) Clayey-silty sequences, *Cl-S*; (d) Clayey-marly sequences, *Cl-M*

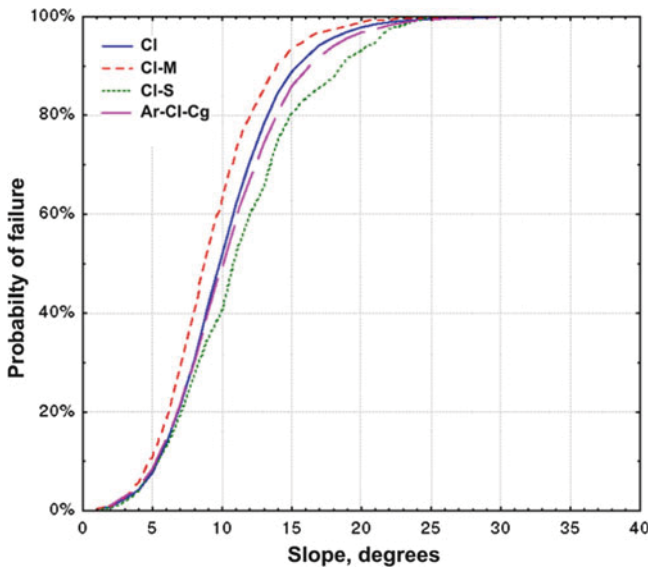


Fig. 7 Cumulative distribution functions of mean slope-angle distributions of landslides for each geological sequence

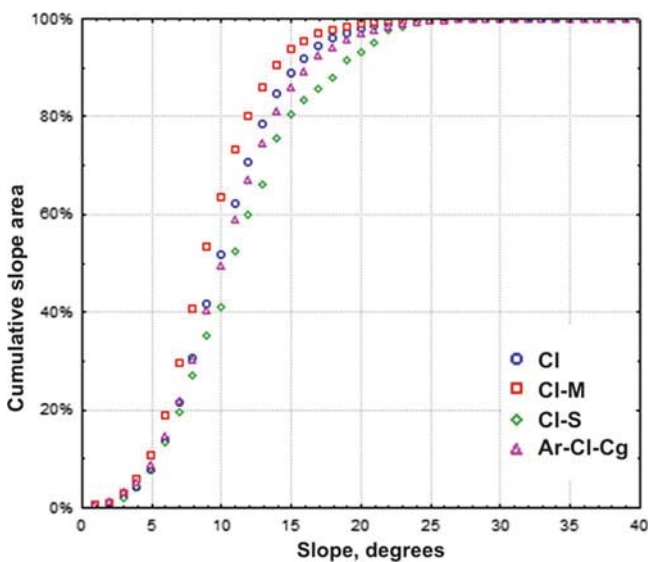


Fig. 8 Cumulative slope angle distribution

shows a unimodal asymmetric shape with peak values generally around 10°.

The cumulative Weibull distribution function $F(A)$ was thus computed for the four litho-technical sequences (Fig. 7). Although the preliminary analysis of the probability of failure curves shows that the model seems to describe well the variability of experimental data, some interpretations should be necessarily made. First, the morpho-structural setting of large-scale areas may influence the slope angles distribution, increasing its variability. Second, the heterogeneous nature and setting of the outcropping sequences play a dominant role in the slope gradient pattern, resulting

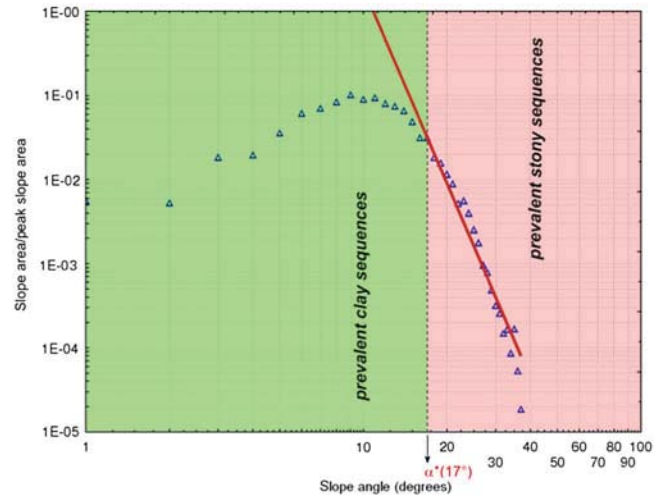


Fig. 9 Distribution curve of the landslide area in relation to the slope angle

in gently slope shapes alternated by rough and steep morphologies. The latter are characterized by a low spatial landslide frequency and, therefore, a lack of materials prone to developing landslides.

Therefore, when operating in geologically complex areas, the probability computed by the Weibull model must be calibrated and interpreted in the specific morphological context. In fact, the cumulative distribution function $C(A)$ (6) shows that more than 95 % of the outcropping of the four litho-technical sequences has slope angles lower than 17° (Fig. 8).

$$C(A) = \sum_{\alpha_i < \alpha} C(A = \alpha_i) \quad (6)$$

This value represents the point of intersection (roll-over, α^*) of two data sets in the bi-logarithmic graph of the slope angle (Fig. 9). In particular, the spatial analysis of α shows that the areal frequency distribution beyond the roll-over is controlled by the following power law equation:

$$y = 2E + 08 - 7.909\alpha \quad (r^2 = 0.96)$$

This correlation is valid for slope angles ranging between 12° < α < 39°.

The value $\alpha^* = 17$ aims at identifying the lower threshold defining slope angles influenced by the outcropping of stony sequences. It is assumed that slopes having a slope angle higher than α^* correspond to sectors where stony layers are outcropping.

In order to adapt the model to the specific study case, the probability of failure curves were recalculated considering the influence of α^* .

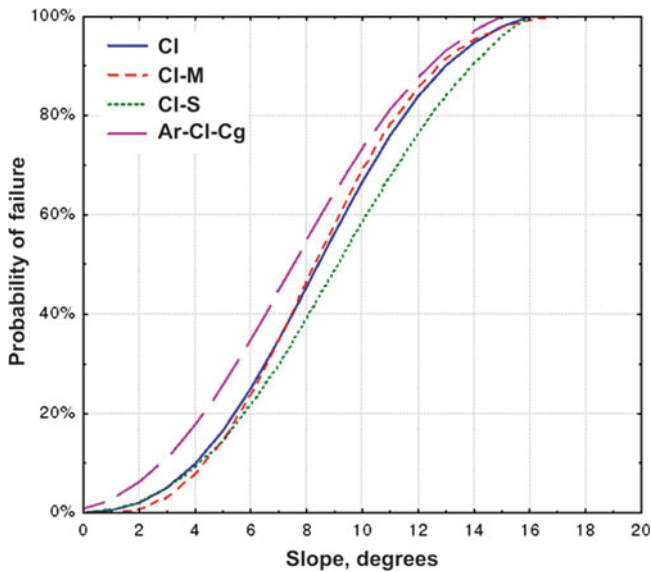


Fig. 10 Curves of probability of failure calculated in relation to the cumulative slope angle distribution

The probability of failure distributions for the four litho-technical sequences is shown in Fig. 10.

Conclusion

The study highlights and confirms that slope angle analysis is a key aspect in landslide susceptibility analysis.

The relationship between landslide frequency and slope angle underlines the role that landslides have in landscape evolution. Generally, slope steepness is significantly influenced by the geological nature of the slope. In the study area the mainly clayey sequences show a good regular Gaussian disposition with peak values, 9–14°, which are included in the shear strength fully-softened to residual range obtained by means of ring shear tests on typical clayey samples (Grelle and Guadagno 2010; Grelle et al. 2011a).

However, the fitting Weibull functions for the four study sequences, CI, Ar-CI-Cg, CI-S and CI-M, show a different pattern which is referable both to the interaction between the geo-structural sequence and the slopes and the retrogressive evolution of landslides, which is typical of source areas.

As reported in the literature, the probability failure analysis by considering slope angles only should take into account the real lithology of the slope. In this study the threshold angle between the low and high stony abundance in the terrain sequences was attributed to the roll-over in the bi-log curve of the landslide area in relation to the slope angle. Consequently, the suitable slope failure analysis was performed again on angles under this threshold.

Finally, it is possible to ascertain that earth flows in the study area, or in similar complex geological areas, are not

immediately connected to the slope angle distribution. For this reason a preliminary, deep knowledge of the study site and a post-processing analysis addressed to contextualize the output data are needed.

The results obtained indicate that accurate slope angle analyses considerably improve landslide susceptibility studies in areas characterized by complex terrains, evaluating its effective contribution as landslide predisposing factor.

References

- Corominas J, Moya J, Ledesma A, Lloret A, Gili JA (2005) Prediction of ground displacements and velocities from groundwater level changes at the Vallcebre landslide (Eastern Pyrenees, Spain). *Landslides* 2(2):83–96
- Environmental Systems Research Institute (ESRI) (1999) Arcview GIS 3.2. Environmental Systems Research Institute Inc, Redlands
- Esu F (1977) Behaviour of slopes in structurally complex formations. In: Proceedings of the international symposium on the geotechnics of structurally complex formations, vol 2. Capri, 292–304
- Grelle G, Guadagno FM (2010) Shear mechanism and viscoplastic effects during impulsive shearing. *Geotechnique* 60(2):91–103
- Grelle G, Revellino P, Guadagno FM (2011a) Methodology for seismic and post-seismic stability assessment of natural clay slopes based on a viscoplastic behaviour model in simplified dynamic analysis. *Soil Dyn Earthq Eng* 31(9):1248–1260. doi:10.1016/j.soildyn.2011.05.005
- Grelle G, Revellino P, Donnarumma A, Guadagno FM (2011b) Bedding control on landslides: a methodological approach for computer-aided mapping analysis. *Nat Hazard Earth Syst Sci* 11:1395–1409. doi:10.5194/nhess-11-1395-2011
- Guadagno FM, Focareta M, Revellino P, Bencardino M, Grelle G, Lupo G, Rivellini G (2006) La carta delle frane della provincia di Benevento. Sannio University Press, Benevento
- Guzzetti F, Ardizzone F, Cardinali M, Galli M, Reichenbach P, Rossi M (2007) Distribution of landslides in the Upper Tiber river basin, Central Italy. *Geomorphology*. doi:10.1016/j.geomorph.2007.07.015
- Iwahashi J, Watanabe S, Furuya T (2001) Landform analysis of slope movements using DEM in Higashikubiki area, Japan. *Comput Geosci* 27(7):851–865
- Iwahashi J, Watanabe S, Furuya T (2003) Mean slope-angle frequency distribution and size frequency distribution of landslide masses in Higashikubiki area, Japan. *Geomorphology* 50:349–364
- Korup O (2005) Distribution of landslides in southwest New Zealand. *Landslides* 2:43–51
- Lee CT, Huang CC, Lee JF, Pan KL, Lin ML, Dong J (2008) Statistical approach to storm event-induced landslides susceptibility. *Nat Hazard Earth Syst Sci* 8:941–960
- Lollino G, Lollino P, Bertolino G (2003) Analysis of the behaviour of a large landslide in structurally complex soils by means of monitoring field data. In: Proceedings of the international conference – Fast slope movements prediction and prevention for risk mitigation – Naples, May 11–13. Vol 1. Ed. Patron. Bologna, pp 317–324
- Ohmori H, Sugai T (1995) Toward geomorphometric models for estimating landslide dynamics and forecasting landslide occurrence in Japanese mountains. *Zeitschrift fur Geomorphologie* 101:149–164, Supplementband
- PWRI (1976) Jisuberi no Jittai-toukei (2) (The actual statistics of landslides no.2): Technical Memorandum of PWRI 1121 (in Japanese)
- Revellino P, Grelle G, Donnarumma A, Guadagno FM (2010) Structurally-controlled earth flows of the Benevento Province (Southern Italy). *Bull Eng Geol Env* 69(3):487–500. doi:10.1007/s10064-010-0288-9

- Weibull W (1951) A statistical distribution function of wide applicability. *J Appl Mech-Trans ASME* 18:293–297
- WP/WLI (1993) A suggested method for describing the activity of a landslide. *Bull of the IAEG* 47:53–57
- Xiaoyi F, Jianping Q (2006) Effect on stratum gradient frequency distribution of landslides in the three gorges area of northeast Chongqing. *Wuhan Univ J Nat Sci* 11(4):767–772. doi:[10.1007/BF02830162](https://doi.org/10.1007/BF02830162)